

Microemulsions as microreactors in physical organic chemistry*

Luis García-Río¹, J. Ramon Leis^{1,‡}, Juan Carlos Mejuto², and Moisés Pérez-Lorenzo¹

¹Departamento de Química Física, Facultad de Química, Universidad de Santiago de Compostela, 15782 Santiago de Compostela, Spain; ²Departamento de Química Física, Facultad de Ciencias, Universidad de Vigo, Ourense, Spain

Abstract: Microemulsions are very versatile reaction media which nowadays find many applications, ranging from nanoparticle templating to preparative organic chemistry. The thermodynamically stable and microheterogeneous nature of microemulsions, used as reaction media, induces drastic changes in the reagent concentrations, and this can be specifically used for tuning the reaction rates. In particular, amphiphilic organic molecules can accumulate and orient at the oil–water interface, inducing regiospecificity in organic reactions. In this review, we will show the recent tendencies of the use of microemulsions as organic reaction media.

Keywords: microemulsions; reactivity; AOT; mechanisms; colloid.

INTRODUCTION

Microemulsions are stable, transparent solutions of water, oil, and surfactant, with or without a cosurfactant. They have been described as consisting of spherical droplets of a disperse phase separated from a continuous phase by a film of surfactant [1]. Because they provide both organic and aqueous environments, microemulsions can simultaneously dissolve both hydrophobic and hydrophilic compounds, each compound being distributed among water, organic solvent, and surfactant film in accordance with its physicochemical properties. Owing to their microheterogeneous structure, microemulsions have found a growing number of scientific and technological applications: They afford control over the size of synthesized microparticles [2], and they have numerous applications in the fields of solubilization and extraction [3,4]. They have been used to simulate complex biological structures (in particular as regards the behavior of trapped water) [5,6]. In keeping with this proliferating range of applications, there is an increasing interest in studying the details of chemical [1a], photochemical [7], and enzymo-catalytic [1a,8] processes in microemulsions. In particular, since microemulsions are able, like phase-transfer catalysis systems, to enhance reactions between non-hydro-soluble organic substrates and hydro-soluble reagents, the kinetics of numerous reactions in microemulsions have been studied [1b,9].

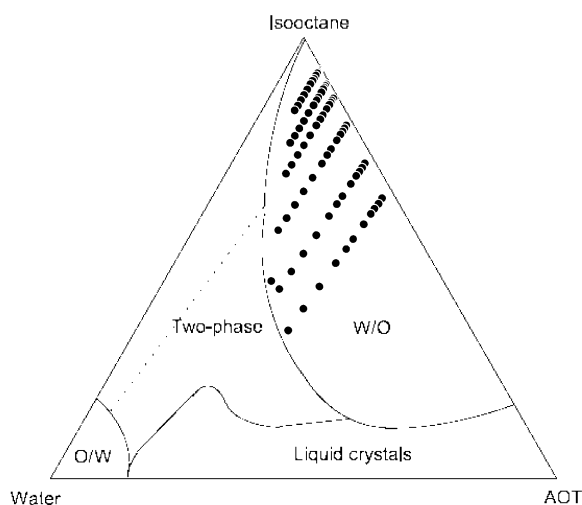
We have developed a kinetic model to quantitatively explain the influence of microemulsions on chemical reactivity [10]. Equivalent expressions to those derived by us were obtained by Casavino and co-workers and applied to iron(III) oxidation of some alkyl-substituted ferrocenes [11] and the kinetics of substitution in palladium(II) complexes [12]. Sánchez et al. have shown that the Brønsted equation,

*Paper based on a presentation at the 18th International Conference on Physical Organic Chemistry (ICPOC-18), 20–25 August 2006, Warsaw, Poland. Other presentations are published in this issue, pp. 955–1151.

‡Corresponding author

which can be derived directly from the transition-state theory, is an alternative to the pseudophase model to rationalize the observed kinetic effects in microemulsions [13].

Most of these studies have been carried out in AOT-based microemulsions, AOT being the sodium salt of bis(2-ethylhexyl)sulfosuccinate. The microemulsion composition will be characterized in terms of two parameters W and Z , which are defined as the molar ratio [water]/[AOT] and [isooctane]/[AOT], respectively. Scheme 1 shows the typical compositions of the water-in-oil (w/o) microemulsions, which have been used to carry out our studies. The microemulsion composition was varied in order to cover a wide interval, where the W composition parameter, $W = [\text{H}_2\text{O}]/[\text{AOT}]$, varies between $W = 2$ –40. Hence, the microemulsions used display a wide variation in properties such as polarity, viscosity, hydrogen-bond donation capacity, saline content, etc.



Scheme 1

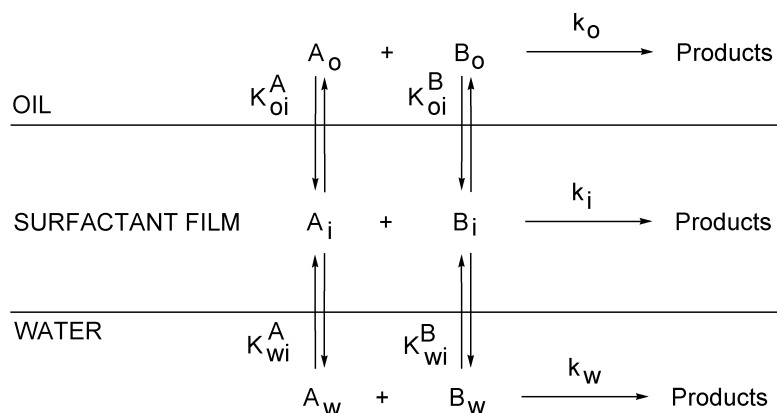
PSEUDOPHASE MODEL

Kinetic studies of reactions in w/o microemulsions can be interpreted in terms of reactivity, only if local reagent concentrations and intrinsic rate constants in the various microphases of these organized media can be obtained from the overall, apparent rate data. Our research group has devised a kinetic model based on the formalism of the pseudophase, which can be applied to carry out a quantitative interpretation of the influence of the composition of the microemulsion on the chemical reactivity [10]. In order to apply this formalism to the basic hydrolysis of the *p*-nitrophenyl acetate (NPA), we need to consider the microemulsion formed by three strongly differentiated pseudophases: an aqueous pseudophase (w), a continuous medium formed fundamentally by the isooctane (o), and an interface formed fundamentally by the surfactant (i). The application of the pseudophase model considers that each pseudophase is uniformly distributed in the total volume of the microemulsion. In view of the solubility characteristics of reactants, their distribution among these pseudophases can be described by partition coefficients. Partition coefficients have been expressed in terms of mole ratios in each phase, a choice that makes the kinetic treatment much easier [10]. Problems and approximations involved in these definitions have been discussed in the literature [14].

For the application of the kinetic treatment, the partitioning reagent distribution along the microenvironments of the microemulsions must be faster than the reaction rate under study. The kinetics of solubilizate exchange between water droplets of a w/o microemulsion have been widely studied by Robinson et al. [15a–b], Fletcher et al. [15c], and Pileni et al. [15d]. Their approach involves an analysis of a reaction in a w/o microemulsion involving reactant species totally confined within the dispersed

water droplets, so that a necessary step prior to their chemical reaction is a transfer of reactants into the same droplet. When the chemical reaction is fast (close to diffusion-controlled), the overall reaction rate is likely to be controlled by the rate of interdroplet transfer or reacting species. The interdroplet transfer rate was measured as a function of the droplet size, the temperature, the surfactant, and the continuous medium. Exchange rates were determined using very fast chemical reactions as indicators for exchange. Three types of reaction were investigated: proton transfer, metal–ligand complexation, and electron transfer. Similar exchange rates were found for all three reactions. For AOT as dispersant, exchange occurs with a second-order rate constant of 10^6 – 10^8 $M^{-1}s^{-1}$, depending on the droplet size and temperature. The exchange rate constants are 2–4 orders of magnitude slower than the droplet encounter rate, as predicted from simple diffusion theory.

The general model (shown in Scheme 2) does not seem to be readily verifiable by means of its full application to a single reaction, since most reactions exhibit the same sort of limitations: (a) insolubility of one or more reagents in one of the pseudophases and (b) great disparity (by several orders of magnitude) between the reaction rates in different pseudophases.



Scheme 2

Considering pseudo-first-order conditions where $[B] \ll [A]$, we can obtain an analytical expression for the observed rate constant, k_{obs} , (1). Subscripts and superscripts w , o , and i , respectively, indicate water, oil, and surfactant film; $[A]_T$ means total reagent concentration as the sum of concentrations in water, oil, and surfactant film pseudophases. \bar{V}_i , \bar{V}_w , and \bar{V}_o are the molar volumes for each pseudophase.

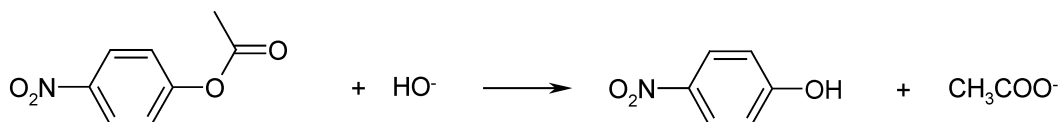
$$k_{obs} = \frac{[A]_T}{[AOT]} \left(\frac{\frac{k_i}{\bar{V}_i} + \frac{\frac{k_w}{\bar{V}_w} W}{K_{wi}^A K_{wi}^B} + \frac{\frac{k_o}{\bar{V}_o} Z}{K_{oi}^A K_{oi}^B}}{1 + \frac{W}{K_{wi}^A} + \frac{Z}{K_{oi}^A}} \right) \left(1 + \frac{W}{K_{wi}^B} + \frac{Z}{K_{oi}^B} \right) \quad (1)$$

Appropriate simplification of this equation allow us to obtain k_{obs} expressions for any reduced model, including all those used to modelize the examples shown in this work [10,16,17].

EXAMPLES OF APPLICATION OF THE PSEUDOPHASE MODEL

Reactions taking place in one phase: Reaction at water

This case is probably the more studied in the literature [9]. Good examples of these kinds of reactions are the basic hydrolysis reactions in AOT-based microemulsions. These reactions should take place in the aqueous nanodroplet because the presence of negative-charged AOT head group implies that the aqueous nanodroplet is the only domain of the microemulsion that is accessible for the hydroxide ions. A typical example is the basic hydrolysis of NPA [18] (Scheme 3)



Scheme 3

The distribution of the reactants through the microemulsion pseudophases, the *loci* of reaction, and the rate equation derived from the kinetic model are shown in Table 1. Application of the model yields a dependence of the bimolecular rate constant for the basic hydrolysis of NPA in the water nanodroplet with the water content of the microemulsion, $W = [\text{H}_2\text{O}]/[\text{AOT}]$ (see Fig. 1). As the water content of the microemulsion decreases, a change occurs in its physical properties which is able to alter chemical reactivity. The observed effect will be a consequence of the desolvation of the hydroxide ion, which entails an increase in reactivity, and the lower degree of solvation of the transition state, with a consequent decrease in the reaction rate. The balance of both factors will allow us to explain the experimental results.

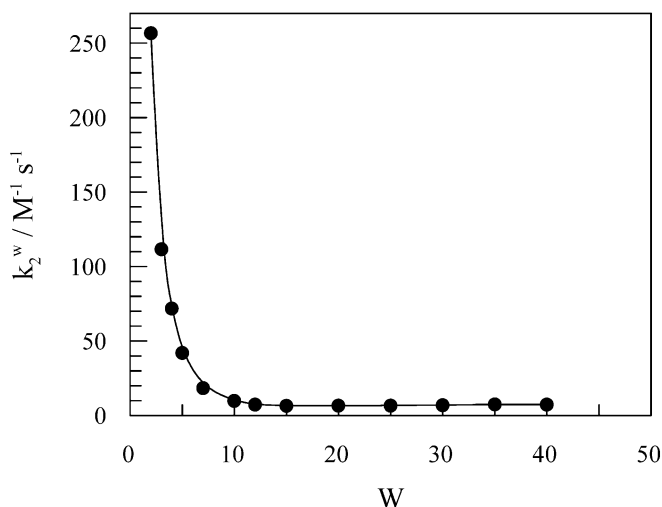


Fig. 1 Influence of W on the bimolecular rate constant in the water domain (k_2^w) for the basic hydrolysis of the NPA in microemulsions of AOT/isooctane/water at 25 °C. $[\text{OH}^-] = 5.00 \times 10^{-2} \text{ M}$ referred to the aqueous medium.

From a quantitative point of view, the desolvation of the hydroxide ion seems to be the greatest contribution to the decrease in activation energy of the reaction. The results obtained for this reaction are consistent with the existence of four types of water [19]: trapped water, bound water (bound to the

Table 1

Reaction	Partition of reactive A			Partition of reactive B			Loci of reaction			Pseudophase equation
	water	surf.	oil	water	surf.	oil	water	surf.	oil	
Hydrolysis	Nitrophenyl acetate (A) + OH ⁻ (B) ¹⁸									$k_{obs} = \frac{[A]}{[AOT]} \left[\frac{k_p W}{V_w} \frac{K_{ot}^A K_{ot}^B}{1 + K_{ot}^A + K_{ot}^B} \left(\frac{W}{K_{ot}^A} + \frac{Z}{K_{ot}^B} \right) \right]$
	Piperazine (A) + MNTS (B) ¹⁰									$k_{obs} = \frac{[A]}{[AOT]} \left[\frac{k_p}{V_f} \left(\frac{W}{1 + K_{ot}^A} + \frac{Z}{1 + K_{ot}^B} \right) \right]$
Nitrosation	NMBA (A) + MNTS (B) ¹⁰									
	Methylethylamine (A) + MNTS (B) ¹⁶									
	Methylbutylamine (A) + MNTS (B) ¹⁶									
	Methylhexylamine (A) + MNTS (B) ¹⁶									$k_{obs} = \frac{[A]}{[AOT]} \left[\frac{k_p}{V_f} \left(\frac{Z}{1 + K_{ot}^A} + \frac{Z}{1 + K_{ot}^B} \right) \right]$
	Methyloctylamine (A) + MNTS (B) ¹⁶									
	Methyldodecylamine (A) + MNTS (B) ¹⁶									
	NMBA (A) + Ethoxy-ethyl nitrite (B) ¹⁷									$k_{obs} = \frac{[A]}{[AOT]} \left[\frac{k_p}{V_f} \left(\frac{Z}{1 + K_{ot}^A} + \frac{Z}{1 + K_{ot}^B} + \frac{Z}{K_{ot}^A} \right) \right]$
	NMBA (A) + Bromo-ethyl nitrite (B) ¹⁷									$k_{obs} = \frac{[A]}{[AOT]} \left[\frac{k_p}{V_f} \left(\frac{Z}{1 + K_{ot}^A} + \frac{Z}{1 + K_{ot}^B} + \frac{Z}{K_{ot}^A} \right) \right]$
	Piperidine (A) + MNTS (B) ¹⁰									$k_{obs} = \frac{[A]}{[AOT]} \left[\frac{k_p}{V_f} \left(\frac{W}{1 + K_{ot}^A} + \frac{Z}{1 + K_{ot}^B} + \frac{Z}{K_{ot}^A} \right) \right]$
	Dimethylamine (A) + MNTS (B) ¹⁰									$k_{obs} = \frac{[A]}{[AOT]} \left[\frac{k_p}{V_f} \left(\frac{W}{1 + K_{ot}^A} + \frac{Z}{1 + K_{ot}^B} + \frac{Z}{K_{ot}^A} \right) \right]$
Morpholine (A) + MNTS (B) ¹⁰									$k_{obs} = \frac{[A]}{[AOT]} \left[\frac{k_p}{V_f} \left(\frac{W}{1 + K_{ot}^A} + \frac{Z}{1 + K_{ot}^B} + \frac{Z}{K_{ot}^A} \right) \right]$	

(continues on next page)

Table 1 (Continued).

Pyrrolidine (A) + MNITS (B) ¹⁰	$k_{obs} = \frac{[A]_p}{[AOT]} \left(\frac{k_i}{V_i} \left(\frac{W}{1 + \frac{K_{wt}^A}{K_{wt}^B}} + \frac{Z}{K_{wt}^B} \right) \left(1 + \frac{Z}{K_{wt}^B} \right) \right)$
Piperazine (A) + Ethoxy-ethyl nitrite (B) ¹⁷	$k_{obs} = \frac{[A]_p}{[AOT]} \left(\frac{k_i}{V_i} + \frac{k_{wt} W}{V_i} \left(\frac{K_{wt}^B}{K_{wt}^A K_{wt}^{wt}} \right) \left(\frac{W}{1 + \frac{K_{wt}^B}{K_{wt}^A}} + \frac{Z}{K_{wt}^B} \right) \right)$
Piperazine (A) + Bromo-ethyl nitrite (B) ¹⁷	$k_{obs} = \frac{[A]_p}{[AOT]} \left(\frac{k_i}{V_i} + \frac{k_{wt} W}{V_i} \left(\frac{K_{wt}^B}{K_{wt}^A K_{wt}^{wt}} \right) \left(\frac{W}{1 + \frac{K_{wt}^B}{K_{wt}^A}} + \frac{Z}{K_{wt}^B} \right) \right)$
Morpholine (A) + Ethoxy-ethyl nitrite (B) ¹⁷	$k_{obs} = \frac{[A]_p}{[AOT]} \left(\frac{k_i}{V_i} + \frac{k_{wt} W}{V_i} \left(\frac{K_{wt}^B}{K_{wt}^A K_{wt}^{wt}} \right) \left(\frac{W}{1 + \frac{K_{wt}^B}{K_{wt}^A}} + \frac{Z}{K_{wt}^B} \right) \right)$
Morpholine (A) + Bromo-ethyl nitrite (B) ¹⁷	$k_{obs} = \frac{[A]_p}{[AOT]} \left(\frac{k_i}{V_i} + \frac{k_{wt} W}{V_i} \left(\frac{K_{wt}^B}{K_{wt}^A K_{wt}^{wt}} \right) \left(\frac{W}{1 + \frac{K_{wt}^B}{K_{wt}^A}} + \frac{Z}{K_{wt}^B} \right) \right)$
Sarcosine (A) + NPA (B) ²⁰	$k_{obs} = \frac{[A]_p}{[AOT]} \left(\frac{k_i}{V_i} + \frac{k_{wt} W}{V_i} \left(\frac{K_{wt}^B}{K_{wt}^A K_{wt}^{wt}} \right) \left(\frac{W}{1 + \frac{K_{wt}^B}{K_{wt}^A}} + \frac{Z}{K_{wt}^B} \right) \right)$
Piperazine (A) + NPA (B) ²⁰	$k_{obs} = \frac{[A]_p}{[AOT]} \left(\frac{k_i}{V_i} + \frac{k_{wt} W}{V_i} \left(\frac{K_{wt}^B}{K_{wt}^A K_{wt}^{wt}} \right) \left(\frac{W}{1 + \frac{K_{wt}^B}{K_{wt}^A}} + \frac{Z}{K_{wt}^B} \right) \right)$
Glycine (A) + NPA (B) ²⁴	$k_{obs} = \frac{[A]_p}{[AOT]} \left(\frac{k_i}{V_i} + \frac{k_{wt} W}{V_i} \left(\frac{K_{wt}^B}{K_{wt}^A K_{wt}^{wt}} \right) \left(\frac{W}{1 + \frac{K_{wt}^B}{K_{wt}^A}} + \frac{Z}{K_{wt}^B} \right) \right)$
N-decylamine (A) + NPA (B) ²⁰	$k_{obs} = \frac{[A]_p}{[AOT]} \left(\frac{k_i}{V_i} + \frac{k_{wt} W}{V_i} \left(\frac{K_{wt}^B}{K_{wt}^A K_{wt}^{wt}} \right) \left(\frac{W}{1 + \frac{K_{wt}^B}{K_{wt}^A}} + \frac{Z}{K_{wt}^B} \right) \right)$
N-methyl-L-benzylamine (A) + NPA (B) ²¹	$k_{obs} = \frac{[A]_p}{[AOT]} \left(\frac{k_i}{V_i} + \frac{k_{wt} W}{V_i} \left(\frac{K_{wt}^B}{K_{wt}^A K_{wt}^{wt}} \right) \left(\frac{W}{1 + \frac{K_{wt}^B}{K_{wt}^A}} + \frac{Z}{K_{wt}^B} \right) \right)$
Morpholine (A) + NPA (B) ²⁵	$k_{obs} = \frac{[A]_p}{[AOT]} \left(\frac{k_i}{V_i} + \frac{k_{wt} W}{V_i} \left(\frac{K_{wt}^B}{K_{wt}^A K_{wt}^{wt}} \right) \left(\frac{W}{1 + \frac{K_{wt}^B}{K_{wt}^A}} + \frac{Z}{K_{wt}^B} \right) \right)$
Piperazine (A) + MEM (B) ²¹	$k_{obs} = \frac{[A]_p}{[AOT]} \left(\frac{k_i}{V_i} + \frac{k_{wt} W}{V_i} \left(\frac{K_{wt}^B}{K_{wt}^A K_{wt}^{wt}} \right) \left(\frac{W}{1 + \frac{K_{wt}^B}{K_{wt}^A}} + \frac{Z}{K_{wt}^B} \right) \right)$

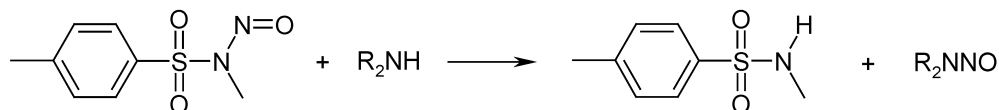
counterion or to the head group of the surfactant), and normal water. These four types of water should coexist and interchange rapidly. The trapped water is found dispersed among the hydrocarbon chains of the surfactant molecules, existing as monomers and dimers, and does not hydrogen-bond with its surroundings. The normal water is found in the center of the aqueous microdroplet and has strong hydrogen-bond interactions. Besides these two types of water, there are other bound water molecules in the vicinity of the ionic tensioactive. The local interactions of the water molecules with the counterions and the head groups of the tensioactive cause opposite effects on the structure of the water. The hydration of the anionic head groups of the tensioactive increases the electronic density on the hydrogen atoms in the water molecules, with the consequent rupture of the hydrogen bonds of the normal water. The intensity of the O–H bonds increases, and this factor means that the chemical displacement of the water protons bonded to the head groups is found in higher fields than the normal water, and the vibration frequency of the O–H bond is found at higher frequencies.

On the other hand, the counterions accumulated in the interior of the aqueous microdroplets can polarize the water molecules, giving rise to a lower electronic density around the protons and consequently a decrease in the strength of the O–H bond of the water. This effect causes a displacement to lower fields of the ^1H NMR resonance signals of the protons of the water, and the frequency of the vibration of the O–H bond is displaced to lower frequencies. This weakening of the strength of the hydrogen bond will contribute to the increase in the desolvation of the hydroxide ion as the water content of the microemulsion decreases and, consequently, the reaction rate increases. Moreover, changes in polarity, pH, and viscosity and altered interfacial rigidity may concertedly act to modify the chemical reactivity in w/o microemulsions when W decreases.

Reactions taking place in one phase: Reaction at AOT film

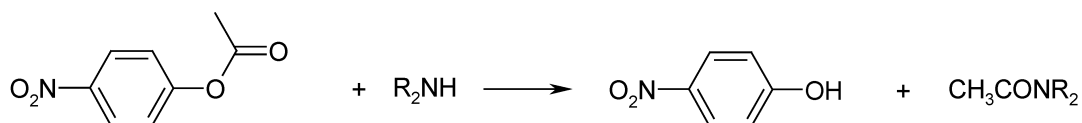
To modelize this situation, we chose the nitrosation of different secondary amines by *N*-methyl-*N*-nitroso-*p*-toluenesulfonamide (MNTS) in water/AOT/isooctane microemulsions [10,16] (see Scheme 4).

The amines were chosen to allow comparisons between amines resident in different phases and between amines with different basicity in water. MNTS is very poorly soluble in water, in fact, solutions of MNTS with as much as 2×10^{-2} M of OH^- (referred to as the total volume of solution) are stable in w/o microemulsions for long periods of time (several days) [10].



Scheme 4

Other examples of this case are the aminolysis of NPA by *n*-decylamine [20] and *N*-methyl-benzylamine [21] (Scheme 5) or the nitrosation of *N*-methyl-benzylamine by ethoxy-ethyl-nitrite and bromo-ethyl-nitrite (RONO) in water/AOT/isooctane microemulsions [17] (see Scheme 4).



Scheme 5

The reagents' distribution, the *loci* of reaction, and the rate equation derived from the kinetic model are shown in Table 1. Comparison of rate constants in the AOT film with those corresponding to reaction in bulk water shows that the nitroso transfer reactions are 20–50 times slower at the interface of the microemulsion, which can be attributed to the lower polarity of the interfacial region. The transition state for our reaction requires a certain degree of charge separation, and reduction of the polarity will cause a decrease in reaction rate [22], as in normal micellar aggregates [23].

Reactions taking place simultaneously in two phases: Reaction at water and AOT film

This mechanism can be illustrated with the reactions of alkyl nitrites (ethoxy-ethyl nitrite and bromo-ethyl nitrite) with piperazine and morpholine [17]. In this case, the nitrosating agent will be present in the three pseudophases while the piperazine will be insoluble in isooctane, hence it will be present only in the water and AOT film pseudophases. The morpholine is soluble in the three pseudophases. As in the previous case, the partition of reactants, the *loci* of reaction, and the kinetic model are shown in Table 1.

The reactions studied proceed much more slowly in the interphase because the polarity of the interface is smaller than in bulk water, but the values obtained in the water pseudophase are compatible with the corresponding one obtained from bulk water. Other reactions that can illustrate this case are the aminolysis of NPA in AOT-based microemulsions by piperazine and sarcosine [20]. In this case, the fit of the pseudophase model equation to the experimental results was satisfactory. When studying the aminolysis of the NPA in AOT-based microemulsions, we found two types of strongly differentiated behavior: the rate constant of the aminolysis in the aqueous microdroplet increases as W decreases (Fig. 2) while the rate constant in the interface increases along with W (Fig. 3).

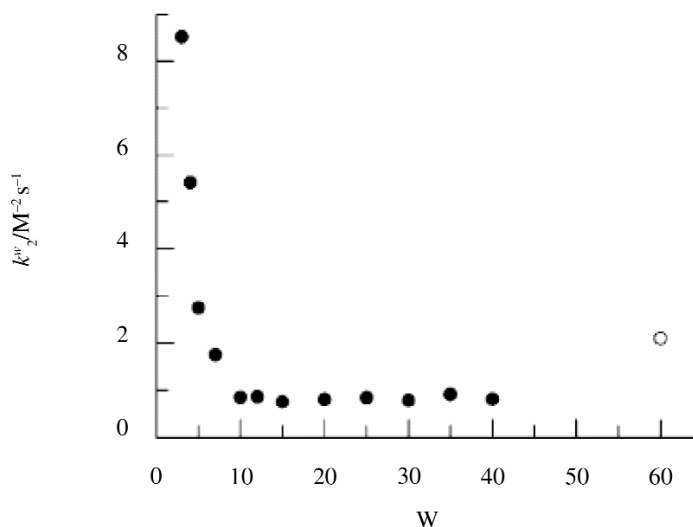


Fig. 2 Influence of W on k^w_2 for the aminolysis of NPA by sarcosine in AOT/isooctane/water microemulsions at 25 °C. (●) $[\text{SAR}] = 5.00 \times 10^{-2} \text{ M}$ referred to the volume of the aqueous microdroplet. Bimolecular rate constant obtained in bulk water (○).

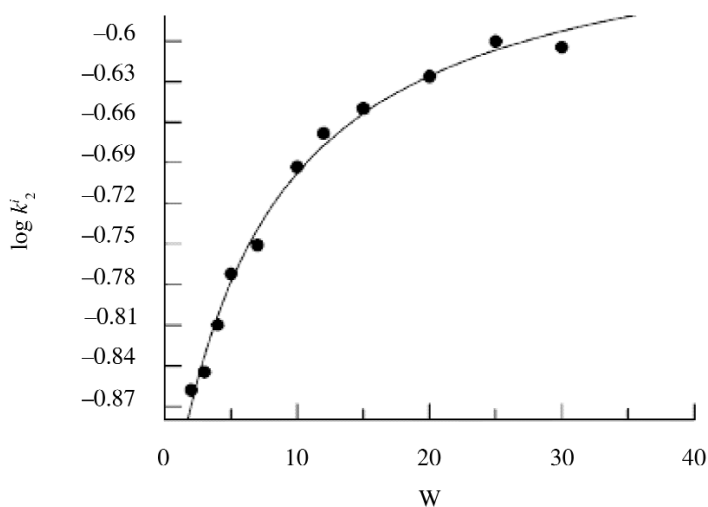
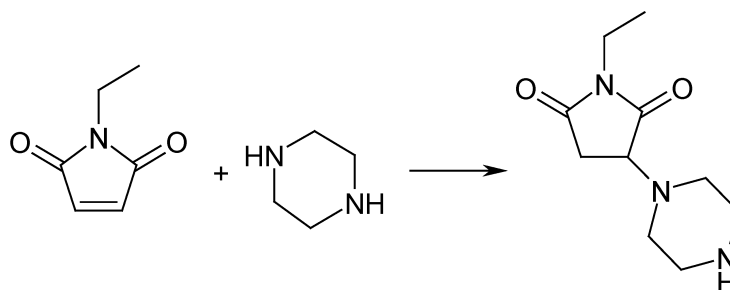


Fig. 3 Influence of W on $\log k'_2$ (bimolecular rate constant for the reaction at the interface) for the aminolysis of NPA by *n*-decylamine in AOT/isooctane/water microemulsions at 25 °C; [DEC] = 2.50×10^{-2} M referred to the total volume of the system.

This change in behavior cannot be attributed to different mechanisms, since it has been shown that the aminolysis mechanism of the NPA in water and in the interface must take place through the formation of an addition intermediate. Therefore, this difference in behavior must be a consequence of the different properties of the water in the aqueous and interfacial microdroplet [19], and of its different capacity for solvation of the reagents and transition states of the reaction.

Another example of this distribution of reactives and reaction *loci* is the Michael addition (Scheme 6) between piperazine and *N*-ethylmaleimide (MEM) [21] and the aminolysis of NPA by glycine [24] and morpholine [25] (Scheme 5).



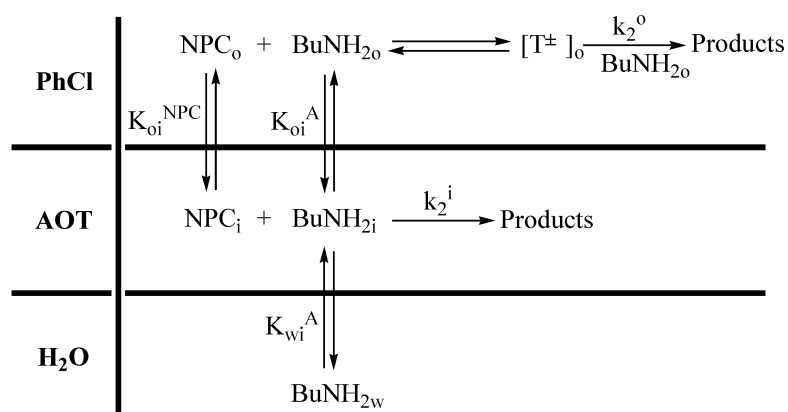
Scheme 6

Reactions taking place simultaneously in two phases: Reaction at AOT film and continuous medium

We have previously studied the aminolysis of NPA by hydrophobic amines in AOT/isooctane/water microemulsions. However, the higher reaction rate at the interface of the microemulsion compared to isooctane, together with a favorable distribution of reactants, caused the reaction to proceed only at the interface. In an attempt to shift the reaction to the continuous medium, the hydrophobic character or the ester was increased by replacing NPA with 4-nitrophenyl caprate (NPC), and the polarity of the continuous medium was increased by replacing isooctane with chlorobenzene. The results obtained [26] by

studying the butylaminolysis of NPC in AOT/chlorobenzene/water microemulsions indicate both first- and second-order dependence on amine concentration, which correspond to the reaction occurring both at the interface and in the continuous medium simultaneously. Nucleophilic attack of butylamine on the ester generates a tetrahedral intermediate, T^\ddagger , whose base-catalyzed decomposition is the rate-determining step in chlorobenzene and is responsible for the second-order term in BuNH_2 . When the polarity of the reaction medium is increased, the formation of the intermediate, T^\ddagger , becomes the rate-determining step, which is made clear by the first-order term in BuNH_2 , corresponding to the process occurring at the interface.

To carry out a quantitative interpretation of the observed behavior, it is necessary to propose a reaction scheme such as those shown in Scheme 7, where the reaction takes place simultaneously at the interface and continuous medium and where the rate-determining step corresponds to the formation and decomposition of T^\ddagger , respectively. The values of the rate constants at the interface and continuous medium indicate that the reaction rate decreases approximately 25 times upon going from the aqueous medium to the interface of the microemulsion, whereas the rate constant in the continuous medium is consistent with that obtained in pure chlorobenzene.

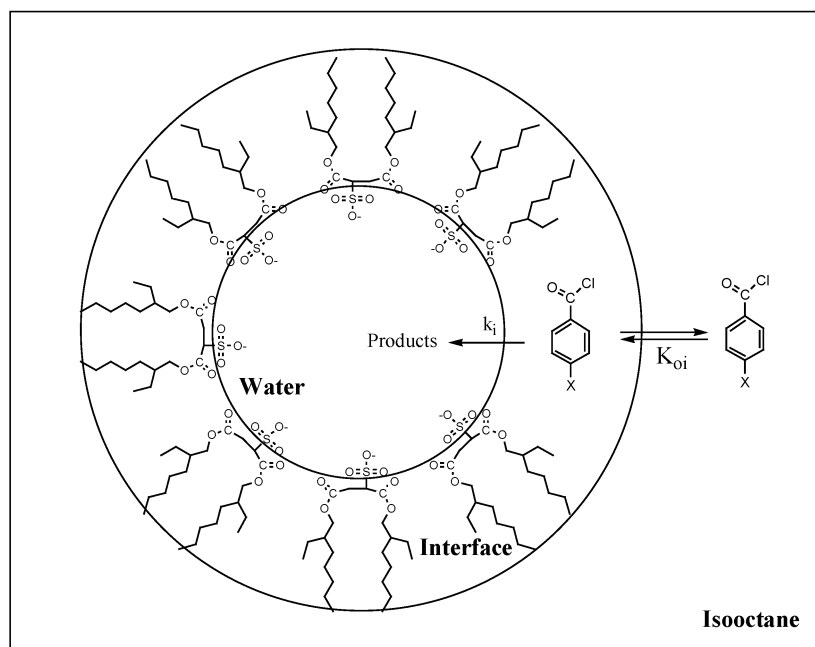


Scheme 7

MICROEMULSION-PROMOTED MECHANISTIC CHANGES

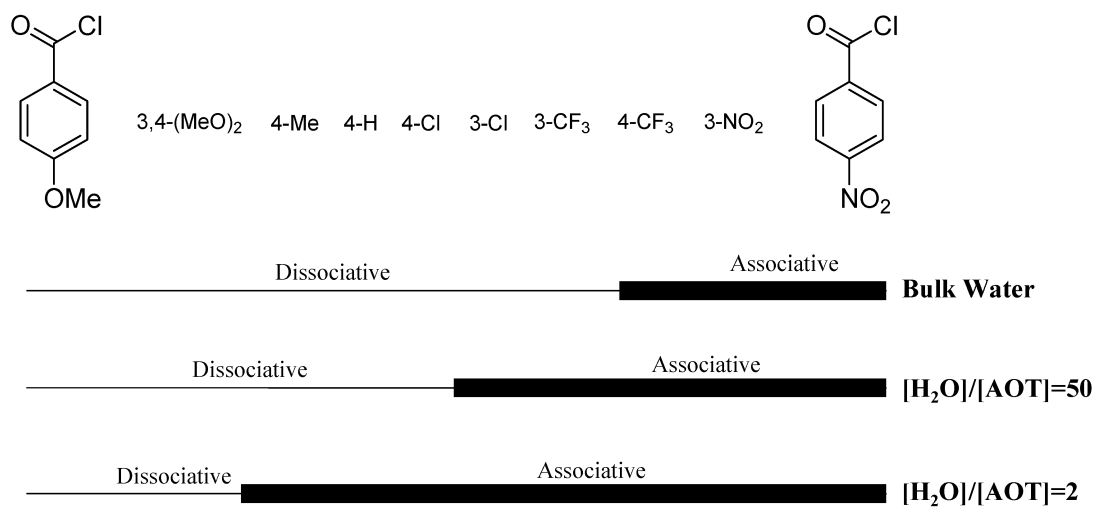
Solvolysis reaction rates are usually written as unimolecular rate constants, and they are the simplest example to be studied in microemulsions. Solvolysis of substituted benzoyl chlorides was studied in AOT/isooctane/water microemulsions [27]. In order to apply the pseudophase model, it was assumed that benzoyl chlorides are only present at the interface and the oil pseudophase. This is quite reasonable, taking into account their low solubility in water. This distribution (Scheme 8) yields to the conclusion that the only pseudophase, where benzoyl chlorides and water are present, is the interface of the microemulsion, and hence the reaction should take place at the interface.

Kinetic results allow several conclusions: (i) reaction rate changes with W as a consequence of the changes of the physical properties of the interface; (ii) the rate constant for high water content, $W \cong 50$, is much lower than in bulk water due to the insufficient hydration of the interface; (iii) the influence of W on the rate constant is determined by the reaction mechanism. For benzoyl chlorides following a dissociative mechanism, the rate constant increases with W while, on the contrary, for associative mechanisms, rate constants increase when W decreases.



Scheme 8

When comparing rates of solvolysis of benzoyl fluoride, chloride, and bromide in AOT-based microemulsions [28], the ratio k_{Br}/k_F decreases 40 times when W decreases from $W = 50$ to $W = 2$. Such decrease of the ratio k_{Br}/k_F agrees with a more efficient associative solvolytic mechanism on decreasing the water content of the microemulsion. As a result, the change of mechanism from a predominately dissociative pathway to an associative one shifts from bulk water to the interface of an AOT-based microemulsion. Moreover, this point also changes on changing the water content of the system. As can be seen in Scheme 9, on decreasing the water content of the microemulsion, the percent of the associative pathway in the solvolysis of substituted benzoyl chlorides increases.



Scheme 9

Recent studies on solvolysis of benzoyl chlorides and 4-nitrophenylchloroformate in CO₂-induced microemulsions [29] of (EO)₂₇(PO)₆₁(EO)₂₇ (P104; EO = ethylene oxide, PO = propylene oxide)/*p*-xylene/CO₂/H₂O show that the observed rate constant of both substrates increase significantly with *W*, and that *W* has a larger influence on the hydrolysis of benzoyl chloride. The different influence of *W* on the two reactions can be explained in terms of the different reaction mechanisms. Studying the decarboxylation reaction of 6-nitrobenzoxazole-3-carboxylate ion (6NBIC) in cetyltripropylammonium bromide (CTPABr) and AOT investigated the relationship between rate constants and water properties in microemulsions in CCl₄ microemulsions [30]. With CTPABr, decarboxylation is much faster than in water, and its addition slows the reaction. The anionic substrate in the interior of CTPABr microemulsions interacts with the CTPA⁺ head group, which assists charge delocalization in the transition state, and reactions at *W* ≅ 0 are faster than those in water by a factor of approximately 10⁶. With AOT, decarboxylation of 6NBIC has a rate similar to that in water and there is no catalysis, with 0 < *W* < 10 indicating that decarboxylation takes place in the water pool and does not involve the anionic surfactant, consistent with repulsive interactions between anionic 6NBIC and the AOT head groups.

ACKNOWLEDGMENTS

Financial support from Ministerio de Ciencia y Tecnología (Project CTQ2005-04779) and Xunta de Galicia (PGIDT03-PXIC20905PN and PGIDIT04TMT209003PR) is gratefully acknowledged.

REFERENCES

1. (a) P. L. Luisi, B. E. Straub (Eds.). *Reverse Micelles*, Plenum Press, New York (1984); (b) M. P. Pileni (Ed.). *Structure and Reactivity in Reverse Micelles*, Elsevier, Amsterdam (1989); (c) M. Zulauf, H. F. Eicke. *J. Phys. Chem.* **83**, 480 (1979).
2. J. H. Fendler. *Chem. Rev.* **87**, 877 (1987).
3. (a) P. Mukerjee, A. Ray. *J. Phys. Chem.* **70**, 2144 (1966); (b) P. Mukerjee, J. R. Cardinal, N. R. Desai. In *Micellization, Solubilization and Microemulsions*, K. L. Mittal (Ed.), Plenum Press, New York (1977).
4. (a) J. Funasaki. *J. Phys. Chem.* **83**, 1998 (1979); (b) M. S. Fernández, P. Fromherz. *J. Phys. Chem.* **83**, 1755 (1977).
5. (a) M. Wong, J. K. Thomas, M. Gräzel. *J. Am. Chem. Soc.* **98**, 2391 (1976); (b) G. Bakale, G. Beck, J. K. Thomas. *J. Phys. Chem.* **85**, 1062 (1981); (c) P. E. Zinsli. *J. Phys. Chem.* **83**, 3223 (1979); (d) E. Keh, B. Valeur. *J. Colloid Interface Sci.* **79**, 465 (1981).
6. (a) J. K. Thomas. *Chem. Rev.* **80**, 281 (1980); (b) W. Marcel. *Proteins: Struct. Funct. Genet.* **1**, 4 (1986).
7. E. A. Lissi, D. Engel. *Langmuir* **8**, 452 (1992).
8. (a) Y. L. Khmel'nitsky, I. N. Neverova, V. I. Polyakov, V. Y. Grinberg, A. V. Levashov, K. Martinek. *Eur. J. Biochem.* **190**, 155 (1990); (b) R. M. D. Verhaert, R. Hilhorst. *Recl. Trav. Chim. Pays-Bas* **110**, 236 (1991).
9. (a) F. M. Menger, J. A. Donohue, R. F. Williams. *J. Am. Chem. Soc.* **95**, 286 (1973); (b) J. M. Blandamer, J. Burges, B. Clark. *J. Chem. Soc., Chem. Commun.* 659 (1983); (c) R. Da-Rocha-Pereira, D. Zanette, F. Nome. *J. Phys. Chem.* **94**, 356 (1990); (d) S. M. Hubig, M. A. J. Rodgers. *J. Phys. Chem.* **94**, 1933 (1990); (e) C. J. O'Coner, E. J. Fendler, J. H. Fendler. *J. Am. Chem. Soc.* **95**, 600 (1973); (f) O. A. El-Seoud, M. J. Da Silva, L. P. Barbur, A. Martine. *J. Chem. Soc., Perkin Trans. 2* 331 (1987); (g) M. Valiente, E. Rodenas. *J. Phys. Chem.* **95**, 3368 (1991); (h) C. Izquierdo, J. Casado. *J. Phys. Chem.* **95**, 6001 (1991); (i) J. R. Leis, J. C. Mejuto, M. E. Peña. *Langmuir* **9**, 889 (1993); (j) C. Gomez-Herrero, M. M. Graciana, E. Muñoz, M. L. Moya, F. Sanchez. *J. Colloid Interface Sci.* **141**, 454 (1991); (k) R. A. Mackay. *Adv. Colloid Interface Sci.* **15**, 131 (1981); (l) C. Minero, E. Pramauro, E. Pelizzetti. *Langmuir* **4**, 101 (1988).

10. L. García-Río, J. R. Leis, M. E. Peña, E. Iglesias. *J. Phys. Chem.* **97**, 3437 (1993).
11. F. P. Cavasino, C. Sbriziolo, M. L. Turco-Liveri. *J. Chem. Soc., Faraday Trans.* **94**, 395 (1998).
12. (a) F. P. Cavasino, C. Sbriziolo, M. L. Turco-Liveri. *J. Phys. Chem. B* **102**, 3143 (1998); (b) F. P. Cavasino, C. Sbriziolo, M. L. Turco-Liveri. *J. Phys. Chem. B* **102**, 5050 (1998).
13. (a) R. Jiménez, M. M. Graciani, A. Rodríguez, M. L. Moyá, F. Sánchez, P. López-Cornejo. *Langmuir* **13**, 187 (1997); (b) F. Sánchez, M. L. Moyá, A. Rodríguez, R. Jiménez, C. Gómez-Herrera, C. Yanes, P. López-Cornejo. *Langmuir* **13**, 3084 (1997); (c) P. López-Cornejo, P. Pérez, F. García, R. de la Vega, F. Sánchez. *J. Am. Chem. Soc.* **124**, 5154 (2002).
14. P. Stilbs. *J. Colloid Interface Sci.* **87**, 385 (1982).
15. (a) P. D. I. Fletcher, A. M. Howe, B. H. Robinson. *J. Chem. Soc., Faraday Trans. 1* **83**, 985 (1987); (b) B. H. Robinson, D. C. Steytler, R. D. Tack. *J. Chem. Soc., Faraday Trans. 1* **75**, 481 (1979); (c) S. Clark, P. D. I. Fletcher, X. Ye. *Langmuir* **6**, 1301 (1990); (d) T. K. Jain, G. Cassin, J. P. Badlali, M. P. Pileni. *Langmuir* **12**, 2408 (1996).
16. L. García-Río, P. Hervés, J. C. Mejuto, J. Pérez-Juste, P. Rodríguez-Dafonte. *Ind. Eng. Chem. Res.* **42**, 5450 (2003).
17. L. García-Río, J. R. Leis, J. C. Mejuto. *J. Phys. Chem.* **100**, 10981 (1996).
18. L. García-Río, J. C. Mejuto, M. Pérez-Lorenzo. *New J. Chem.* **28**, 988 (2004).
19. (a) T. K. Jain, M. Varshney, A. Maitra. *J. Phys. Chem.* **93**, 7409 (1989); (b) Q. Li, S. Weng, J. Wu, N. Zhou. *J. Phys. Chem. B* **102**, 3168 (1998).
20. L. García-Río, J. C. Mejuto, M. Pérez-Lorenzo. *Chem. Eur. J.* **11**, 4361 (2005).
21. E. Fernández, L. García-Río, J. C. Mejuto, M. Pérez-Lorenzo. *New J. Chem.* **29**, 1594 (2005).
22. (a) A. Castro, J. R. Leis, M. E. Peña. *J. Chem. Soc., Perkin Trans. 2* 1861 (1989); (b) L. García-Río, E. Iglesias, J. R. Leis, M. E. Peña, A. Ríos. *J. Chem. Soc., Perkin Trans. 2* 29 (1993).
23. P. D. I. Flecher, A. M. Howe, B. H. Robinson. *J. Chem. Soc., Faraday Trans. 1* **83**, 985 (1987).
24. L. García-Río, J. C. Mejuto, M. Pérez-Lorenzo. *Colloid Surface Sci. A* **270–271**, 115 (2005).
25. L. García-Río, J. C. Mejuto, M. Pérez-Lorenzo. *J. Colloid Interface Sci.* **301**, 624 (2006).
26. L. García-Río, J. C. Mejuto, M. Pérez-Lorenzo. *J. Phys. Chem. B* **110**, 812 (2006).
27. L. García-Río, J. R. Leis, J. A. Moreira. *J. Am. Chem. Soc.* **122**, 10325 (2000).
28. L. García-Río, J. R. Leis, J. C. Mejuto. *Langmuir* **19**, 3190 (2003).
29. R. Zhang, J. Liu, J. He, B. Han, W. Wu, T. Jiang, Z. Liu, J. Du. *Chem. Eur. J.* **9**, 2167 (2003).
30. C. A. Bunton, A. Garreffa, R. Germani, G. Onori, A. Santucci, G. Savelli. *Prog. Colloid Polym. Sci.* **118**, 103 (2001).